JOURNAL OF AGRICULTURAL AND FOOD CHEMISTRY

Properties of Aged Montmorillonite−Wheat Gluten Composite Films

IDOIA OLABARRIETA,[†] MIKAEL GÄLLSTEDT,[§] IBAN ISPIZUA,[#] JOSE-RAMON SARASUA,[#] AND MIKAEL S. HEDENQVIST*,[†]

School of Chemical Science and Engineering, Fiber and Polymer Technology, Royal Institute of Technology, SE-100 44 Stockholm, Sweden; STFI-Packforsk, Packaging and Logistics, Box 5604, SE-114 86 Stockholm, Sweden; and Department of Materials Science, Engineering Faculty, University of Basque Country, 48013 Bilbao, Spain

The properties of new and aged glycerol-plasticized vital wheat gluten films containing ≤4.5 wt % natural or quaternary ammonium salt modified montmorillonite clay were investigated. The films were cast from pH 4 or pH 11 ethanol/water solutions. The films, aged for ≤120 days, were characterized by tensile testing, X-ray diffraction, and transmission electron microscopy. In addition, water vapor permeability (11% relative humidity) and the content of volatile components were measured. The large reduction in the water vapor permeability with respect to the pristine polymer suggests that the clay platelets were evenly distributed within the films and oriented preferably with the platelet long axis parallel to the film surface. The film prepared from pH 11 solution containing natural clay was, as revealed by transmission electron microscopy and X-ray diffraction, almost completely exfoliated. This film was consequently also the strongest, the stiffest, and the most brittle and, together with the pH 11 film containing modified clay, it also showed the greatest decrease in water vapor permeability. The large blocking effect of the clay had no effect on the aging kinetics of the films. During aging, the pH 4 and pH 11 film strength and the pH 4 film stiffness increased and the pH 4 film ductility decreased at the same rate with or without clay. This suggests that the aging was not diffusion rate limited, that is, that the loss of volatile components or the migration of glycerol or glycerol/wheat gluten phase separation was not limited by diffusion kinetics. The aging rate seemed to be determined by slow structural changes, possibly involving protein denaturation and aggregation processes.

KEYWORDS: Wheat gluten; aging; montmorillonite; cast films; tensile properties; water vapor permeability

INTRODUCTION

Composites with specific compositions and structures on a nanometer scale have been shown, over the past 15 years, to possess remarkable property enhancements relative to conventionally scaled composites (*1*). Polymer nanocomposites have received considerable attention since the discovery that polymer properties may be greatly improved by the presence of nanosized particles (*2*). Recent advances in polymer/clay and polymer/layered silicate nanocomposite materials (*1*, *3*, *4*) have inspired efforts to disperse clay-based fillers in almost every common polymer, in the hope of achieving complete exfoliation of the inorganic fillers and consequently obtaining a maximum improvement in performance (*5*).

Degradable and renewable polymers are no exceptions (*6*). However, only a few studies have been reported on renewable polymer/clay nanocomposites. The properties of polylactide, starch, and chitosan clay mixtures have been documented (*6*−*9*), but there are almost no references to protein−clay nanocomposites (*10*).

Due to its high gas barrier properties and, compared to other natural polymers, relatively hydrophobic nature, wheat gluten (WG) is an interesting alternative to synthetic plastics in, for example, food-packaging applications. It is a viscoelastic material with good adhesive, cohesive, and film-forming properties, and it is renewable and biodegradable (*11*).

Several studies deal with the film-forming properties of WG proteins, mostly from water−ethanol dispersions (*12*−*18*). High protein solubility is required to achieve solution-cast films with sufficient quality. The protein solubility and unfolding in water−ethanol mixtures increase with a reduction of the intra- and intermolecular disulfide and hydrogen bonds and a reduction of the hydrophobic interactions. The film and film-forming properties have been shown to depend on the pH of the dispersion. According to Gennadios et al. (*19*), Gontard et al. (*20*), and Pommet et al. (*21*), a pH below 5 or above 10.5 yields a homogeneous film-forming solution that can be cast into films.

To avoid a brittle film, a plasticizer, for example, glycerol, is added to WG. Unfortunaltely, the plasticizer tends to migrate

* Author to whom correspondence should be addressed (telephone +46 8 790 76 45; fax +46 8 20 88 56; e-mail mikaelhe@polymer.kth.se).
[†] Royal Institute of Technology.
[§] STFI-Packforsk.
[#] University of Basque Country.

10.1021/jf0522614 CCC: $33.50
Published on Web 01/31/2006

to the surrounding media and/or phase separate within the film, and this leads to embrittlement (*22*−*24*).

As reported by Olabarrieta et al. (*25*), the largest mechanical changes during aging (decrease in ductility, increase in stiffness and strength) were observed for WG films generated from an acidic solution (pH 4), whereas films prepared from basic solutions (pH 11) were more stable. The changes were attributed to the loss of plasticisers. The results suggested that a low degree of denaturation and low protein aggregation (pH 4) were ineffective in retaining volatile components and glycerol within the film.

In the present investigation, montmorillonite clay has been added to WG. The idea is that the impermeable clay platelets will increase the tortuosity and thereby reduce the aging rate by reducing the loss of volatile components and migrating plasticizers and also increase the WG barrier properties against gases and liquids. Unmodified sodium-rich and quaternary ammonium salt modified montmorillonite clays were used. The unmodified clay was used because it is hygroscopic and is expected to delaminate, at least to a certain degree, in the water−ethanol casting solution. The modified clay was used to see the effects on delamination properties of having a clay that was already expanded. The composite films were characterized in terms of their tensile properties, moisture content, and water vapor permeability. Their structures were determined by X-ray diffraction and transmission electron microscopy.

EXPERIMENTAL PROCEDURES

Materials. The WG powder was kindly supplied by Reppe AB, Lidköping, Sweden. The powder consisted of 84.8 wt % WG proteins, 8.1 wt % wheat starch, 5 wt % water, 1.34 wt % fat, and 0.76 wt % ash. Glycerol with a purity of 99.5% was supplied by Karlshamns Tefac AB, Karlshamn, Sweden. Ethanol (95%) was obtained from Kemetyl AB. Acetic acid (99%) was supplied by Merck Eurolab. Sodium hydroxide was supplied by Sigma Aldrich Chemie, GmbH.

Two types of commercial nanoclay were used: Cloisite Na+ and Cloisite 10A, obtained from Southern Clay Products Inc.. Cloisite Na+ is a natural sodium-rich montmorillonite. Cloisite 10A is a natural montmorillonite modified with a quaternary ammonium salt, $N(CH_3)(CH_3)(CH_2C_6H_5)(HT)^+Cl^-$. Dimethyldihydrogenated tallow (HT) is a mixture of ∼65% C18, ∼30% C16, and ∼5% C14 alkanes. The density of pure montmorillonite is 2608 kg/m^3 (*26*). The amount of ammonium salt in Cloisite 10A was 38 wt % determined by heating the clay isothermally for 10 min at 850 °C using a Mettler-Toledo TGA-SDTA 851 thermobalance.

Methods. *Film Formation.* The films were produced by first stirring 18 g of WG powder and 6 g of glycerol in 90 g of ethanol. After a homogeneous solution had been attained, 60 g of deionized water was added slowly. Consequently, the mass ratio of water and ethanol was 1:1.5. pH 4 and pH 11 solutions were obtained by adding, respectively, acetic acid and sodium hydroxide. The solutions were thereafter heated to 75 °C for 20 min (2.5 °C/min). Ethanol solutions with 0.75, 1.5, 3, and 4.5 wt % natural and modified clay were prepared (the mass percentage refers to the gluten and clay contents in the final film). The corresponding volume concentrations of pure clay, that is, neglecting the surface coating, were 0.28, 0.57, 1.16, and 1.77 vol % in the case of natural clay and 0.18, 0.35, 0.71, and 1.07 vol % in the case of modified clay. These values were calculated from the weight concentrations by assuming that the density of the surface coating was the same as the density of the clay free glycerol−WG film, determined to be ∼1.306 g cm^{-3}. The solutions were ultrasonicated for 3 min with an Elma Ultrasonic T420(H) machine, Elma GmbH & Co. KG, operating at 3.5 kHz and 70 W. Subsequently, the solutions were poured into the 70 °C gluten solution and then stirred for 10 min. Films of 300−400 μm thickness were obtained by pouring the solutions into Petri dishes. The solution was dried for 2 days at 23 °C and 50% relative humidity. The Petri dishes were coated with a release agent layer of poly(tetrafluoroethylene) supported by an aluminum foil (Bytac Type AF-21; Norton Performance Plastics Corp., Wayne, NJ). The film produced from a pH 4 solution was referred to as the pH 4-nat or pH 4-mod film depending on whether it contained natural or modified clay, respectively. The corresponding nomenclature for films prepared at pH 11 was pH 11-nat and pH 11-mod.

Aging of Films. Films were conditioned in a climate chamber at 23 °C and 50% relative humidity for 48 h and then placed, with the side that had faced the Petri dish down, on a porous paper support (Blotting Paper 1600, 220 diameter, from VWR International). The films were aged at 23 °C and 50% relative humidity.

Film Thickness. Film thickness was measured using a Mitutoyo 10C-1128 micrometer (Mitutoyo Scandinavia AB). The mean thickness was calculated from measurements taken at five different locations on each film sample.

Equilibrium Volatile Content at 50% Relative Humidity. The loss of volatile components was measured as described in ASTM D 644-94. The test pieces were weighed and then stored for 24 h at 105 °C in a Nûve FN400 oven, supplied by LabRum Klimat AB. The specimens were subsequently cooled in desiccators at 0% relative humidity and 23 °C and then weighed to determine the loss of volatile components. Three replicates from each sample were measured.

Tensile Testing. The WG films were tensile tested at 50% relative humidity and 25 °C. The specimens were conditioned in this environment for at least 48 h before testing. A Zwick Z010 tensile tester controlled by the testXpert 7.1 computer program supplied from Zwick GmbH & Co. was used. The samples were punched to a dumb-bell shape with a length and width of the narrow section of, respectively, 16.0 ± 1.0 and 4.0 ± 0.1 mm [ISO 37:1994(E)]. The measurements were performed as described in ASTM 882-01 with a crosshead speed of 100 mm/min and a clamp distance of 40 mm. Ten replicates of each sample were measured.

Water Vapor Permeability. The water vapor transmission rate (WVTR) was measured on three replicates of each material using a Mocon Permatran-W Twin (Minneapolis, MN) according to ASTM F 1249-90. Water vapor permeabilities were evaluated using 11% relative humidity on the upstream side and 0% relative humidity on the downstream side of the film. Specimens were tightly sandwiched between two pieces of aluminum foil, leaving a 5 cm^2 exposure area. Before the measurements, the specimens were conditioned for 2 days in isolated diffusion cells with one side in contact with an atmosphere of a saturated LiCl solution (11% relative humidity) and the other side facing dry nitrogen gas.

X-ray Diffraction (XRD). X-ray diffractograms of films were obtained in a Siemens D5000 diffractometer with Cu radiation (50 kV, 40 mA). The scanning speed and the step size were 0.15°/min and 0.02°, respectively. The specimen rotation speed was 15 rpm.

Transmission Electron Microscopy (TEM). The clay−polymer structure was studied by TEM using a Philips Tecnai 10 electron microscope. Samples were embedded in epoxy, and ∼50 nm thick sections were cut at cryogenic temperature (−80 or −120 °C) using an RMC ultramicrotome. The sections were wiped from the diamond knife onto Formvar/carbon-coated Cu grids using a hairpin. Alternatively, after heating to room temperature, the sections were collected from the knife with a water droplet coated grid.

RESULTS AND DISCUSSION

Figures 1−**3** show that the addition of clay to the WG had no effect on the kinetics of aging. The pH 4 film showed the same rate of increase in stiffness, strength, and decrease in ductility as was observed in the reference system without clay. The effect of clay on the pH 11 film, which even without clay did not age dramatically, was negligible.

As shown in **Figures 1**−**3** (3 and 9 day values), the effect of clay on the properties of relatively new films (≤9 days) was modest, the pH 11-nat film being the strongest, stiffest, and most brittle of them all. The modest change was due to the small amount of clay in the films (4.5 wt % = ∼1−2 vol %). The choice of clay content was based on the idea of allowing the individual clay platelets to orient independently and thereby allowing for a more complete exfoliation.

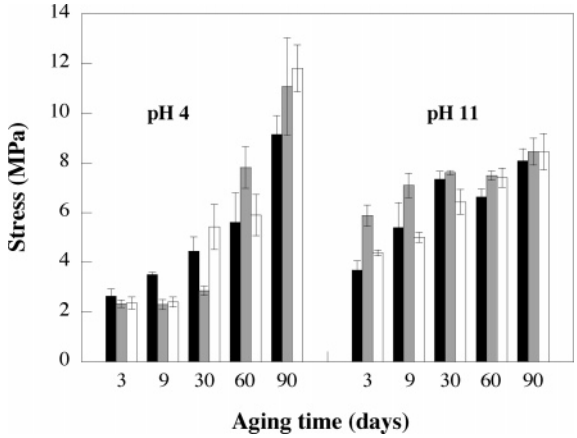

Figure 1. Maximum stress versus aging time for (black bars) WG film, (gray bars) WG film with 4.5 wt % natural clay, and (white bars) WG film with 4.5 wt % modified clay.

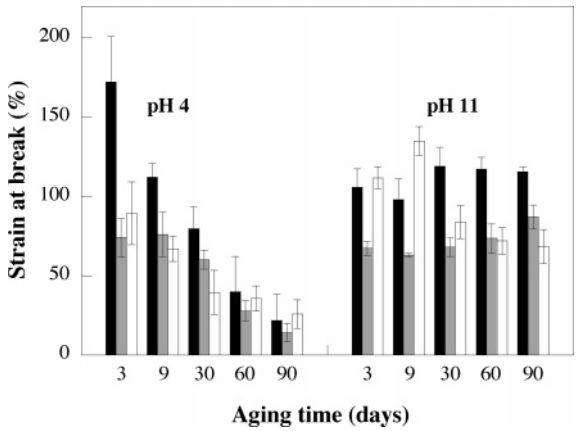

Figure 2. Strain at break (percent) versus aging time for (black bars) WG film, (gray bars) WG film with 4.5 wt % natural clay, and (white bars) WG film with 4.5 wt % modified clay.

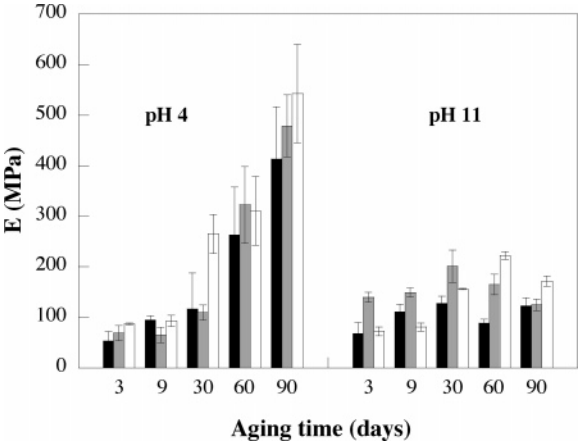

Figure 3. Young's modulus (MPa) versus aging time for (black bars) WG film, (gray bars) WG film with 4.5 wt % natural clay, and (white bars) WG film with 4.5 wt % modified clay.

The maximum clay volume content for independent rotation/orientation can be estimated by considering that this corresponds to a system saturated with spheres, each containing a single clay platelet with circular lateral shape. Inside the sphere the platelet is free to rotate, and the sphere defines its "rotational volume" (**Figure 4a**). The calculated volume fraction (maximum clay volume content) is the ratio of the platelet volume, assuming a platelet thickness of 1 nm, to the volume of the sphere. The maximum clay volume contents for independent rotation/orientation of clay platelets perfectly distributed within the matrix, having an aspect ratio of, respectively, 100, 200, or 400, are 1.5, 0.75, and 0.38 vol %. If the platelet was instead oriented with its long axis within ±45° to the long axis of the film, the values were, respectively, 2.3, 1.1, and 0.6 vol % (**Figure 4b**). Here it was assumed that one platelet shared the sphere section, defined by its orientation of ±45° to the film long axis, with two adjacent platelets (**Figure 4b**). Consequently, the volume fraction in this case is the platelet volume divided by three-fourths of the sphere section. The calculations show, for steric reasons, that it is probable that intact stacks of clay platelets or intercalated tactoids will exist together with exfoliated structures if the clay content is "high", even for a "well-exfoliating" system. The calculations also indicate that the clay platelets, for steric reasons, must be somewhat oriented, at least within limited regions.

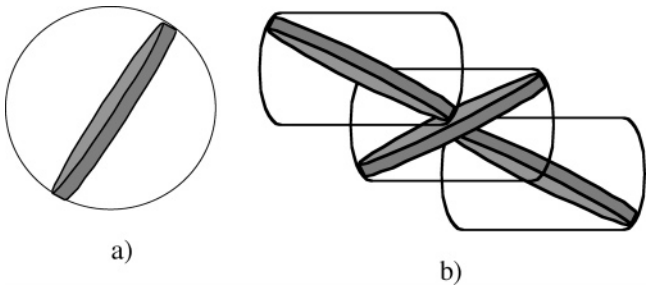

Figure 4. Schematic drawing showing the principles for calculating the maximum volume content of clay for (**a**) free rotation and (**b**) free rotation within ±45° with respect to the long axis of the film.

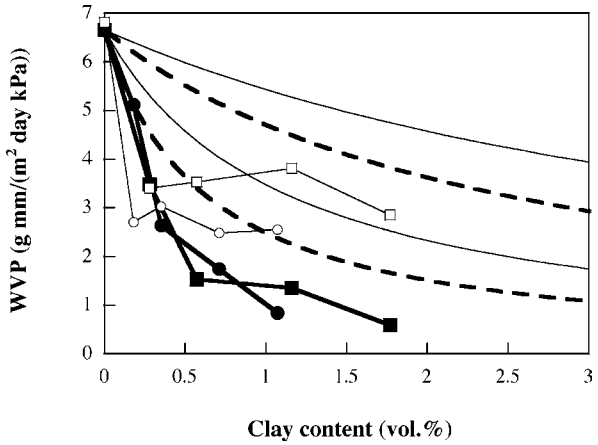

Figure 5. Water vapor permeability as a function of clay content for pH 11-mod (●), pH 11-nat (■), pH 4-mod (○), and pH 4-nat (□) films. Solid lines represent the Fricke model (eqs 1–3) using aspect ratios of 100 (upper curve) and 600 (lower curve). The dashed lines correspond to the model of Fredrickson and Bicerano (eqs 1 and 4) using aspect ratios of 100 (upper curve) and 600 (lower curve). The pH 11 decrease in the permeability was the only significant trend within a 95% confidence limit (Student's *t* test).

To see whether the small content of clay chosen was the reason why there was no effect on the aging kinetics, water vapor permeation data were obtained. The reason to choose a low moisture gradient (11% relative humidity) was to be able to selectively detect the magnitude of geometrical blocking imposed by the impenetrable clay platelets, thus without having to deal with material changes and non-Fickian behavior associated with swelling (*7*, *27*). **Figure 5** shows that the small amount of clay had a great effect on the water vapor barrier properties. It should be noted, because of experimental scatter, that only the pH 11 permeabilities above 0.75 wt % clay were significantly different from the 0 wt % WG permeability within a 95% confidence limit (Student's *t* test).

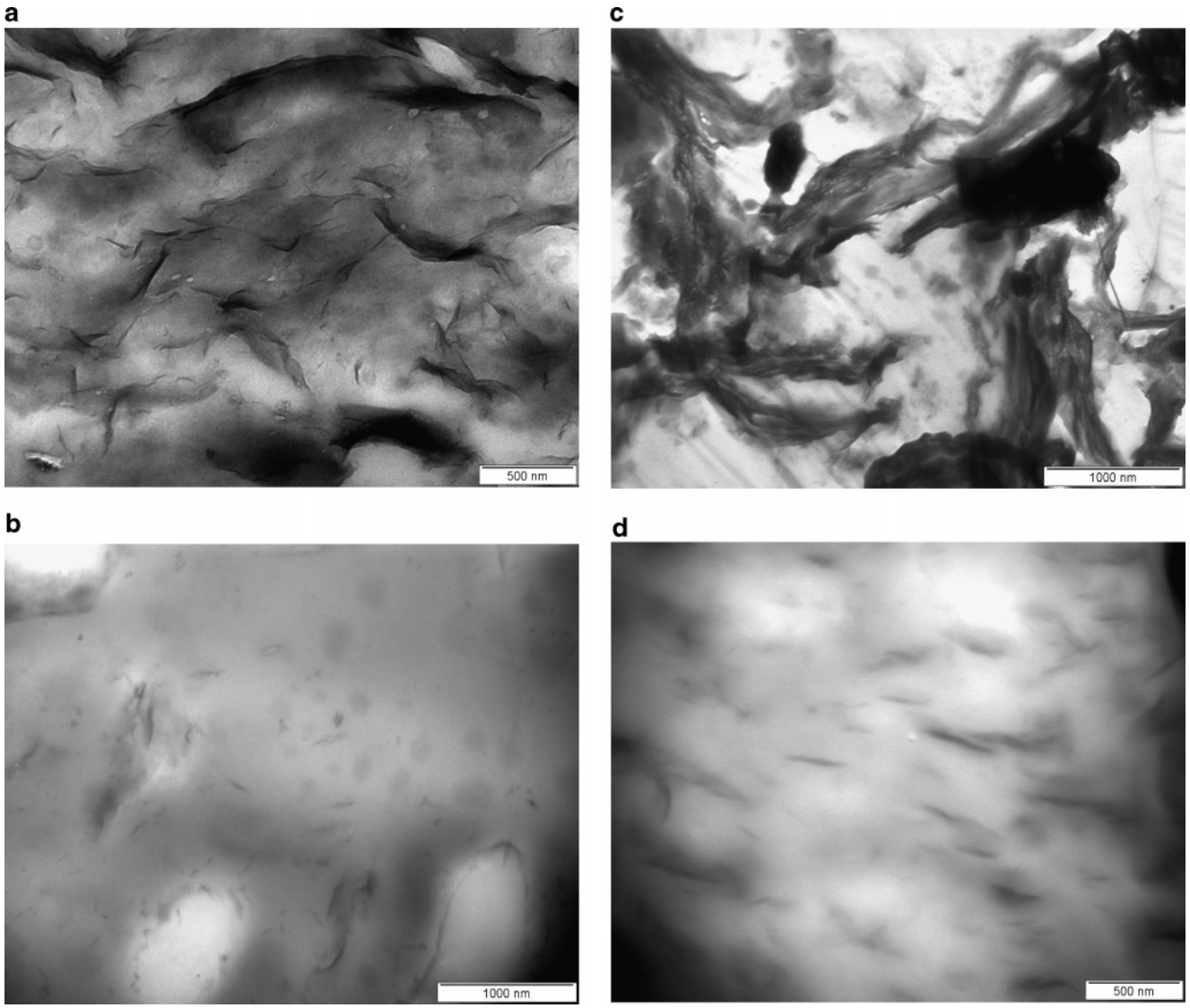

Figure 6. Transmission electron micrographs of (**a**) the pH 11-nat film (4.5 wt % clay), (**b**) the pH 11-mod film (4.5 wt % clay), (**c**) the pH 4-nat film (4.5 wt % clay), and (**d**) the pH 4-mod film (4.5 wt % clay).

The permeability of the composite film was modeled by first considering the platelets as oblate randomly oriented exfoliated spheroids uniformly distributed within the matrix (*28*, *29*). The permeability of the clay−WG film (P_c) is

$$P_c = \frac{P_m \upsilon_m}{\tau} \quad (1)$$

where P_m is the permeability of the polymer matrix and υ_m is the volume fraction of the matrix in the composite. τ is the tortuosity factor, which increases with increasing geometrical blocking of the filler. Provided that the montmorillonite platelets were completely delaminated and that the reduction in permeability was a function solely of the content of filler and its width (w) and thickness (l), the tortuosity factor could be estimated using the relationship

$$X = \frac{1 - \upsilon}{\tau - 1} \quad (2)$$

where X is obtained from

$$\frac{w}{l} = \frac{1}{0.785 - \sqrt{0.616 - \frac{X}{X+3}}} \quad (3)$$

The drop in water permeability was, at least for the pH 11 films, greater than the predicted drop even with a suggested clay platelet aspect ratio as high as 600 (**Figure 5**). As observed in **Figure 6**, most clay platelet widths were within 100−600 nm, and, provided the platelets were exfoliated, the corresponding aspect ratios were consequently 100−600 nm (clay platelet thickness ≈ 1 nm). It is not probable, for gravitational and surface energy reasons, that the upper surface of the drying film will have clay platelets with their long axis perpendicular to the film surface, that is, platelets "standing up" and even pointing out from the film surface. Consequently, during casting, these platelets become oriented with the long axis parallel to the film long axis and force the rest of the platelets below to adopt the same orientation. Indeed, panels **a** and **d** of **Figure 6** indicate that the orientation of individual platelets was not completely random. Consequently, the model based on geometrical blocking developed by Fredrickson and Bicerano (*30*), based on the simple relationship derived by Nielsen (*31*), was used. It is claimed to be an appropriate model for a system in which all clay platelets are oriented with the long axis parallel to the film

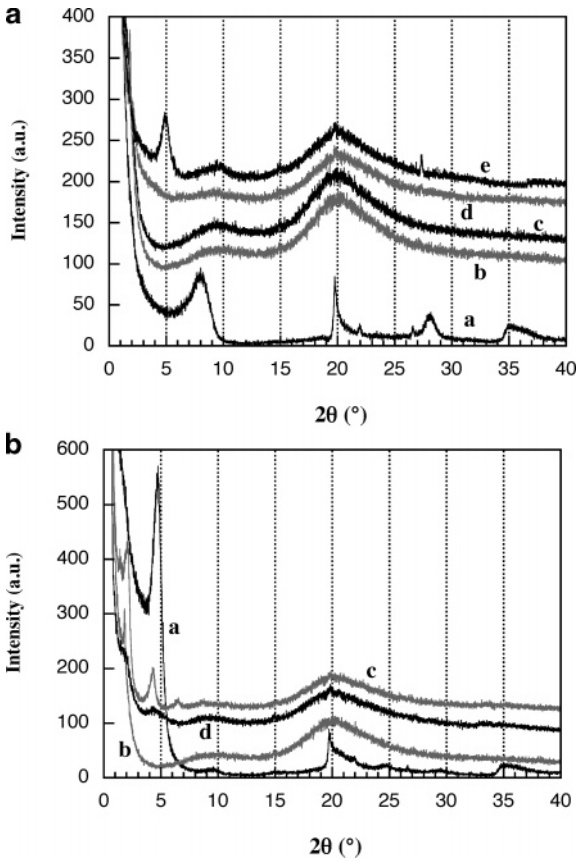

Figure 7. (**a**) XRD spectra of (a) natural clay, (b) WG pH 11, (c) WG pH 4, (d) pH 11-nat (4.5 wt % clay), and (e) pH 4-nat (4.5 wt % clay). (**b**) XRD spectra of (a) modified clay, (b) WG pH 11, (c) pH 11-mod (4.5 wt % clay), and (d) pH 4-mod (4.5 wt % clay).

long axis and in which the clay−polymer system is "dilute", that is, $(w/2l) \times [\pi/\ln(w/(2l))]v_{clay} \leq 3$. Consequently, at the highest contents of clay used, "dilute" means that the aspect ratio must be, respectively, ≤600 and ≤1100 nm in the natural and modified clay systems. The tortuosity is given by

$$\tau = 1 + \frac{w}{2l}\frac{\pi}{\ln\left(\frac{w}{2l}\right)}v_{clay} \quad (4)$$

Figure 5 shows that the experimental water vapor permeabilities were within or below the curves corresponding to eqs 1 and 4 with aspect ratios of 100 and 600. Consequently, it appears that the casting process was beneficial in the sense that clay platelets orient with their long axis parallel to the film long axis. In addition, even though tactoids could be observed in some systems (**Figure 6c**), it appeared that exfoliated clay structures were a common feature in all systems.

Although TEM revealed that exfoliated clay was a common feature (**Figure 6**), XRD showed that the d-001 reflections, indicative of the presence of clay tactoids, were present in all but the pH 11-nat films (**Figure 7**). The d-001 reflections are located at $2\theta \approx 8°$ for pure natural clay and at $2\theta \approx 5°$ for pure modified clay. The tactoids were swollen, as shown by the shift of the d-001 reflection to smaller angles. TEM and XRD indicated that the pH 11-nat film was almost fully exfoliated. In contrast, TEM revealed the presence of tactoids in the pH 4-nat film, and a prominent d-001 reflection was observed in its XRD spectrum (**Figures 6c and 7a**). Nevertheless, the drop in water vapor permeability suggested that this film also contained exfoliated structures. Evidently the pH 11 solution yielded the most efficient delamination of clay, which also explains why the pH 11-nat film had the highest stiffness and strength. This film, together with the pH 11-mod film, also showed the greatest decrease in water vapor permeability. It may be argued that the excess of hydroxyl groups at pH 11 interacts with the surfaces of sodium-rich clay, and to some extent also with the modified clay, in a way that causes the platelets to delaminate. In the case of the pH 11-mod film, the lower affinity of modified clay to moisture was also important for the reduction in its water vapor permeability. **Table 1** shows that the content of volatile components (water, ethanol) at short times (9 days), exemplified by the pH 4 system, was higher in the films with natural clay and that the films with modified clay had a smaller volatile content than the clay-free film.

Table 1. Volatile Contents of pH 4 Films

	volatile content (wt %)		
storage time (days)	pH 4 film	4.5 wt % clay pH 4-nat film	4.5 wt % clay pH 4-mod film
9	17.2 (0.2)[a]	18.4 (0.4)	16.2 (0.6)
30	15.5 (0.9)	17.0 (0.4)	17.5 (0.1)
60	13.5 (0.2)	15.1 (0.2)	12.7 (0.2)
90	9.5 (0.8)	12.3 (1.1)	10.3 (0.4)
120	10.5 (0.1)	10.2 (0.2)	11.1 (1.0)

[a] Values within parentheses are standard deviations.

The fact that the kinetics of aging was unaffected, even though the clay platelets imposed a large geometrical impedance in the film, indicated that the aging was not primarily a diffusion-controlled process. Instead, it seemed that the changes in the protein structure, that is, time-dependent denaturation, aggregation, and protein polymerization during storage, observed especially for the pH 4 film in the previous investigation, determined the rate of loss of volatile components and the glycerol migration/phase separation. It has been shown that both methanol and water solubility decrease with increasing protein aggregation (*32*). It is probable that the driving force for aging, at least to a certain degree, is the rejection of volatiles and plasticizer from the aggregating protein. In addition, it was observed that the migration/diffusion of glycerol and methanol was lower at higher protein aggregation. Consequently, as shown in the previous investigation (*25*), it seems that a higher degree of initial denaturation/aggregation (pH 11) favors a low initial content of volatile components and better retains the plasticizer within the film during aging. In contrast, a low initial degree of aggregation (pH 4) leads to a higher initial content of volatile components but a relatively strong decrease in volatile and plasticizer content during additional aging (time-dependent aggregation).

In conclusion, the water vapor permeability values indicate that the clay platelets effectively acted as geometrical obstacles in the wheat gluten matrix. An important finding was that basic conditions were effective in delaminating the clay platelets. Both TEM and XRD revealed that the pH 11 film containing natural clay provided an almost fully exfoliated structure. The aging kinetics were, however, unaffected by the incorporation of clay, indicating that the aging was not limited by diffusion/migration rates of volatile components and plasticizer. Instead, it was suggested, referring to the time-induced protein changes observed in the previous investigation (*25*), that the slow denaturation and aggregation of the protein, especially prominent in the pH 4 film, was the rate-limiting step in film aging.

ACKNOWLEDGMENT

Martin Svensson and Kurt Villwock from Svenska Lantmännen AB, Sweden, are acknowledeged for valuable discussions. Bo Johansson, Reppe AB, is thanked for supplying the gluten powder, and Alf Svensson, Karlshamns Tefac AB, is thanked for supplying glycerol.

LITERATURE CITED

(1) LeBaron, P. C.; Wang, Z.; Pinnavaia, T. J. Polymer-layered silicate nanocomposites: an overview. *Appl. Clay Sci.* **1999**, *15*, 11−29.

(2) Krook, M.; Albertsson, A. C.; Gedde, U. W.; Hedenqvist, M. S. Barrier and mechanical properties of montmorillonite/polyesteramide nanocomposites. *Polym. Eng. Sci.* **2002**, *42*, 1238−1246.

(3) Giannelis, E. P.; Krishnamoorti, R.; Manias, E. Polymer-silicate nanocomposites: model systems for confined polymers and polymer brushes. *Adv. Polym. Sci.* **1999**, *138*, 107−147.

(4) Alexandre, M.; Dubois, P. Polymer-layered silicate nanocomposites: preparation, properties and uses of a new class of materials. *Mater. Sci. Eng., R* **2000**, *R28*, 1−63.

(5) Manias, E.; Strawhecker, K.; Touny, A.; Wu, L.; Kuppa, V. Concurrent enhancement of various materials properties in polymer/clay nanocomposites. *Proc. Am. Soc. Comput., Tech. Conf.* **2001**, *16*, 236−246.

(6) Darder, M.; Colilla, M.; Ruiz-Hitzky, E. Biopolymer-clay nanocomposites based on chitosan intercalated in montmorillonite. *Chem. Mater.* **2003**, *15*, 3774−3780.

(7) Lagaron, J. M.; Cabedo, L.; Cava, D.; Feijoo, J. L.; Gavara, R.; Gimenez, E. *Food Addit. Contam.* **2005**, *22*, 994−998.

(8) Pluta, M.; Paul, M.-A.; Alexandre, M.; Dubois, P. Plasticized. *J. Polym. Sci., Part B: Polym. Phys.* **2005**, *44*, 299−311.

(9) Huang, M.-F.; Yu, J.-G.; Ma, X.-F. Studies on the properties of montmorillonite-reinforced thermoplastic starch composites. *Polymer* **2004**, *45*, 3157−3162.

(10) Zheng, J. P.; Li, P.; Ma, Y. L.; De Yao, K. Gelatin/montmorillonite hybrid nanocomposite. I. Preparation and properties. *J. Appl. Polym. Sci.* **2002**, *86*, 1189−1194.

(11) Lens, J.-P.; L. A., G.; Stevels, W. M.; Dietz, C. H. J. T.; Verhelst, K. C. S.; Vereijken, J. M.; Kolster, P. Influence of processing and storage conditions on the mechanical and barrier properties of films cast from aquous wheat gluten dispersions. *Ind. Crops Prod.* **2003**, *17*, 119−130.

(12) Kayserilioglu, B. S.; Stevels, W. M.; Mulder, W. J.; Akkas, N. Mechanical and biochemical characterization of wheat gluten films as a function of pH and co-solvent. *Starch/Staerke* **2001**, *53*, 381−386.

(13) Ali, Y.; Ghorpade, V. M.; Hanna, M. A. Properties of thermally-treated wheat gluten films. *Ind. Crops Prod.* **1997**, *6*, 177−184.

(14) Anker, C. A.; Foster, G. A., Jr.; Loader, M. A. Preparing gluten-containing films and coatings. U.S. Patent 3653925, 1972.

(15) Aydt, T. P.; Weller, C. L.; Testin, R. F. Mechanical and barrier properties of edible corn and wheat protein films. *Trans. ASAE* **1991**, *34*, 207−11.

(16) Gennadios, A.; Weller, C. L. Edible films and coatings from wheat and corn proteins. *Food Technol.* **1990**, *44*, 63−9.

(17) Gontard, N.; Guilbert, S.; Cuq, J. L. Water and glycerol as plasticizers affect mechanical and water vapor barrier properties of an edible wheat gluten film. *J. Food Sci.* **1993**, *58*, 206−211.

(18) Herald, T. J.; Gnanasambandam, R.; McGuire, B. H.; Hachmeister, K. A. Degradable wheat gluten films: preparation, properties and applications. *J. Food Sci.* **1995**, *60*, 1147−50.

(19) Gennadios, A.; Brandenburg, A. H.; Weller, C. L.; Testin, R. F. Effect of pH on properties of wheat gluten and soy protein isolate films. *J. Agric. Food Chem.* **1993**, *41*, 1835−1839.

(20) Gontard, N.; Guilbert, S.; Cuq, J.-L. Edible wheat gluten films: Influence of the main process variables on film properties using response surface methodology. *J. Food Sci.* **1992**, *57*, 190−199.

(21) Pommet, M.; Redl, A.; Morel, M.-H.; Guilbert, S. Study of wheat gluten plasticization with fatty acids. *Polymer* **2003**, *44*, 115−122.

(22) Park, H.-M.; Li, X.; Jin, C.-Z.; Park, C.-Y.; Cho, W.-J.; Ha, C.-S. Preparation and properties of biodegradable thermoplastic starch/clay hybrids. *Macromol. Mater. Eng.* **2002**, *287*, 553−558.

(23) Anker, M.; Stading, M.; Hermansson, A.-M. Aging of whey protein films and the effect on mechanical and barrier properties. *J. Agric. Food Chem.* **2001**, *49*, 989−995.

(24) Hernandez-Muñoz, P.; López-Rubio, A.; del Valle, V.; Almenar, E.; Gavara, R. Mechanical and water barrier properties of glutenin films influenced by storage time. *J. Agric. Food Chem.* **2004**, *52*, 79−83.

(25) Olabarrieta, I.; Gällstedt, M.; Sarasua, J.-R.; Johansson, E.; Hedenqvist, M. S. Aging properties of films of plasticized vital wheat-gluten cast from acidic and basic solutions. *Biomacromolecules* **2005**, submitted for publication.

(26) Grim, R. E. *Clay Mineralogy*, 2nd ed.; McGraw-Hill: New York, 1968.

(27) Gennadios, A.; Weller, C. L.; Testin, R. F. Modification of physical and barrier properties of edible wheat gluten-based films. *Cereal Chem.* **1993**, *70*, 426−429.

(28) Fricke, H. A mathematical treatment of the electric conductivity and capacity of disperse systems. *Phys. Rev.* **1924**, *24*, 575.

(29) Krook, M.; Morgan, G.; Hedenqvist, M. S. Barrier and mechanical properties of injection molded montmorillonite/polyesteramide nanocomposites. *Polym. Eng. Sci.* **2004**, *45*, 135−141.

(30) Fredrickson, G. H.; Bicerano, J. Barrier properties of oriented disk composites. *J. Chem. Phys.* **1999**, *110*, 2181−2188.

(31) Nielsen, L. E. Models for the permeability of filled polymer systems. *J. Macromol. Sci. (Chem.)* **1967**, *A1*, 929−942.

(32) Gällstedt, M.; Mattozzi, A.; Johansson, E.; Hedenqvist, M. S. Transport, mechanical and storage properties of compression molded wheat gluten films. *Biomacromolecules* **2004**, *5*, 2020−2028.

Received for review September 13, 2005. Revised manuscript received December 16, 2005. Accepted December 20, 2005. Västsvenska Lantmännens Research Foundation (VL-stiftelsen) is acknowledged for financial support.

JF0522614